

# Measurement of the three-dimensional mirror parameters by polarization imaging applied to catadioptric camera calibration

Olivier Morel, Ralph Seulin, David Fofi \*

## ABSTRACT

A new efficient method of calibration for catadioptric sensors is presented in this paper. It is based on an accurate measurement of the three-dimensional parameters of the mirror by means of polarization imaging. While inserting a rotating polarizer between the camera and the mirror, the system is automatically calibrated without any calibration patterns. Moreover it permits to relax most of the constraints related to the calibration of the catadioptric systems. We show that contrary to our system, the traditional methods of calibration are very sensitive to misalignment of the camera axis and the symmetry axis of the mirror. From the measurement of three-dimensional parameters, we apply the generic calibration concept to calibrate the catadioptric sensor. The influence of the disturbed measurement of the parameters on the reconstruction of a synthetic scene is also presented. Finally, experiments prove the validity of the method with some preliminary results on three-dimensional reconstruction.

## 1. INTRODUCTION

Conventional perspective cameras have limited fields of view that make them restrictive in some applications such as robotics, videosurveillance and so on. A way to enhance the field of view is to place a mirror with surface of revolution in front of the camera so that the scene reflects on the mirror omnidirectionally. Such a system, composed of both lenses (dioptric) and mirrors (catoptric) for image formation, is called catadioptric. Several configurations exist, and those satisfying the Single View Point constraint are described in.<sup>1</sup>

Catadioptric vision systems available on the market have been deeply studied. Commercial devices are not adapted to our requirements as optical components need to be placed between the camera and the mirror. Mirrors have therefore been produced in our own facilities thanks to the Plateform3D department<sup>†</sup>. A high speed machining centre has been used to produce very high quality surface which is then polished.

We developed a new approach of calibrating catadioptric sensor by polarization imaging. This method enables to calibrate all mirror shapes since it is based on the measurement of the three-dimensional parameters such as: height and normals orientations of the surface. The only constraint is that an orthographic camera has to be used. To calibrate the system we apply the generic calibration concept developed by Sturm and Ramalingam.<sup>2,3</sup>

The article is structured as follows. Next section reminds previous work on paracatadioptric calibration since the measurement of the surface normals by polarization imaging induces orthographic projection. We show the misalignment sensitivity of these methods for the reconstruction of a synthetic scene. Then, after presenting some basic knowledge about polarization imaging, we detail how to calibrate the sensor with the generic calibration concept. In section 4, simulations are presented to illustrate the influence of the parameters measurement on the quality of the reconstruction. Preliminary results on a calibrated spherical mirror are also described. Finally, the paper ends with a conclusion and a few words about future work to be undertaken.

---

<sup>†</sup>This work was supported by the A.N.R. (“Agence Nationale de la Recherche”), Ca.Vi.A.R. (Catadioptric Vision of Aerial Robots), project n°NT05-2\_41786. Website: <http://www.anr-caviar.org/>.

<sup>†</sup><http://www.plateform3d.com>

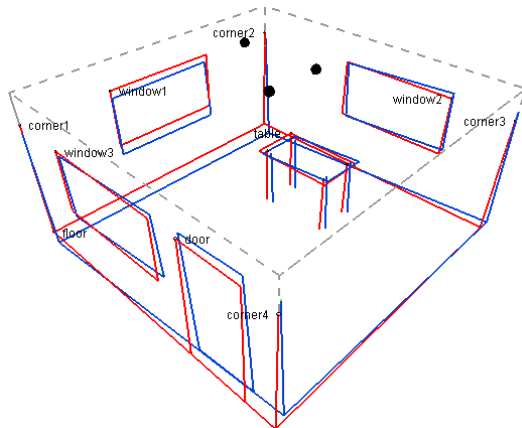


**Figure 1.** Simulation of the three-dimensional reconstruction: the theoretical scene, in blue, represents a room with elements such as windows, door and table ; black dots depict the three locations of the sensor. The reconstructed scene with the Vanderportaele calibration method (misalignment of  $2^\circ$ ) is drawn in red.

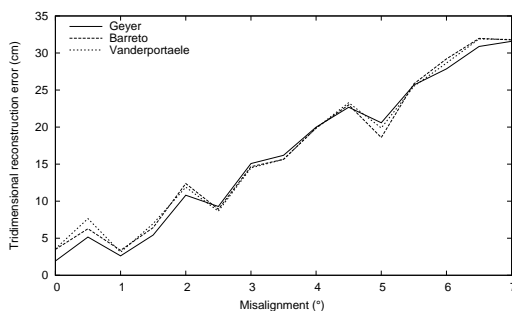


**Figure 2.** Reconstruction error induced by the misalignment between the optical axis of the camera and the symmetry axis of the paraboloid. Calibration method used are Geyer, Barreto and Vanderportaele. (room of size  $500 \times 500 \times 250cm$ )

## 2. CATADIOPTRIC CAMERAS CALIBRATION

### 2.1. Previous work

The most obvious used calibration method is an approach based on the image of the mirror's bounding circle.<sup>4,5</sup> It has the main advantage of being easily automated, but the drawbacks are that the mirror is constructed properly and the mirror boundary accurately encodes the intrinsic parameters. In the field of paracatadioptric camera calibration, more robust methods are based on the fitting of lines projected onto the mirror.<sup>6-8</sup> This approach has also some shortcomings: lines have to be precisely detected and the optical axis of the camera is assumed aligned with the symmetry axis of the paraboloid. To illustrate the misalignment effect, the three-dimensional reconstruction of a synthetic scene based on the calibration of the three preceding methods is simulated (Figure 1).

The scene represents a room of size  $500 \times 500 \times 250cm$  with elements such as windows, doors and table. 3 images of the catadioptric sensor are used to triangulate the points of the scene. For the calibration process, 20 lines are computed and perfectly detected on the mirror. Then the calibration parameters are used to reconstruct the scene (reconstruction made with the linear-eigen method). As we can see on Figure 2 the misalignment of the paracatadioptric system leads to introduce important error on the reconstruction even if the calibration is made with perfect fitting of the lines.

### 2.2. The generic calibration concept

The previous calibration methods for omnidirectional catadioptric sensors assume that: (i) the mirror shape is perfectly known; (ii) the alignment of the sensor is perfect so that the single viewpoint constraint is satisfied;

(iii) the projection model can be easily parametrized. Some methods relax the second constraint and a few relax the first, but before some recent works<sup>2,9,10</sup> calibrating methods always underlie an explicit parametric model of projection. This new model has the advantage of working for any type of camera (catadioptric systems, central cameras with or without distortion, axial cameras, etc.) and to handle heterogeneous systems<sup>3</sup> (for instance, a sensor composed of an omnidirectional camera and a perspective camera). However, developing an efficient and easy-to-use calibration method based on this model is not trivial. In this paper, a proposed new method enables catadioptric sensor calibration by polarization imaging. It relaxes the three constraints listed above ((i), (ii), (iii)). Moreover, the calibration can even be performed by a non-specialist as it only requires an optical apparatus and no image processing.

### 3. POLARIZATION IMAGING

Polarization imaging enables to study the polarization state of a light wave. The most common applications in artificial vision are the abilities to distinguish objects of dielectric and metallic nature<sup>11</sup> and to detect transparent surfaces. Polarization imaging enables likewise to give three-dimensional information of specular objects (“Shape from polarization” method<sup>12,13</sup>). Physical principle is the following: after being reflected, an unpolarized light wave becomes partially linearly polarized, depending on the surface normal and on the refractive index of the media it impinges on. A partially linearly polarized light has three parameters: the light magnitude  $I$ , the degree of polarization  $\rho$  and the angle of polarization  $\varphi$ .

To calibrate the mirror used in our catadioptric sensor, the polarization state of the reflected light has to be measured. A rotating polarizer placed between the camera and the mirror is used. The complete sensor (mirror and camera) and the polarizer are placed into a cylinder made of paper sheet (Fig. 3). Each light intensity of pixels is linked to the angle of the polarizer and to the polarization parameters by the following equation:

$$I_p(\alpha) = \frac{I}{2} (\rho \cos(2\alpha - 2\varphi) + 1), \quad (1)$$

where  $\alpha$  is the polarizer angle. The purpose of polarization imaging is to compute the three parameters,  $I$ ,  $\varphi$ , and  $\rho$ , by interpolating this formula. Because there are three parameters, at least three images, taken with different orientations of the polarizer, are required. To get an automatic calibration of the catadioptric system, a liquid-crystal polarization rotator is used instead of the polarizer. It acts as a rotating polarizer, which has the ability to be electrically controlled. Fig 4 shows the image of the degree and the angle of polarization of a spherical mirror.

#### 3.1. Relationship between the polarization parameters and the normals

Wolff and Boulton have demonstrated how to determine constraints on surface normals by using the Fresnel reflectance model.<sup>14</sup> The surface of the mirror is assumed to be continuous and described by a Cartesian expression:  $z = f(x, y)$ . Therefore, each surface normal is given by the following non-normalized expression:

$$\vec{n} = \begin{bmatrix} -\frac{\partial f(x,y)}{\partial x} \\ -\frac{\partial f(x,y)}{\partial y} \\ 1 \end{bmatrix} = \begin{bmatrix} p = \tan \theta \cos \phi \\ q = \tan \theta \sin \phi \\ 1 \end{bmatrix}. \quad (2)$$

The aim of “Shape from polarization” is to compute the normals from the angles  $\theta$  and  $\phi$ . By combining Fresnel formulas and the Snell-Descartes law one can find a relationship between the degree of polarization  $\rho$  and the zenith angle  $\theta$ .<sup>13</sup> For specular metallic surfaces, the following formula can be applied:<sup>15</sup>

$$\rho(\theta) = \frac{2n \tan \theta \sin \theta}{\tan^2 \theta \sin^2 \theta + |\hat{n}|^2}, \quad (3)$$

where  $\hat{n} = n(1 + i\kappa)$  is the complex refractive index of the mirror.

The azimuth angle  $\phi$  is linked to the angle of polarization  $\varphi$  since the reflected light becomes partially linearly polarized according to the normal of the plane of incidence. Because our imaging system uses a telecentric lens,

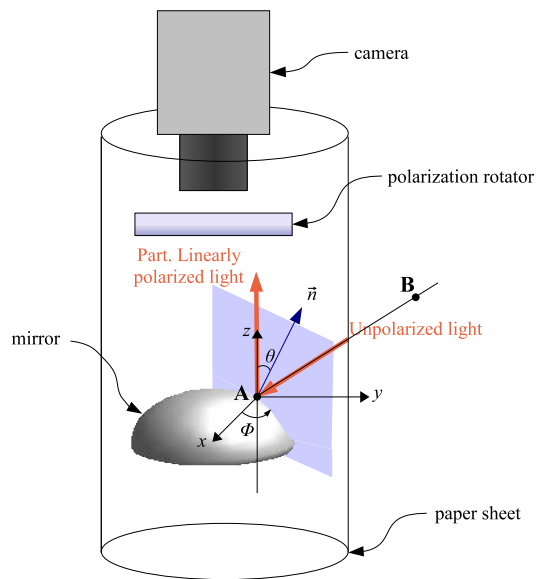
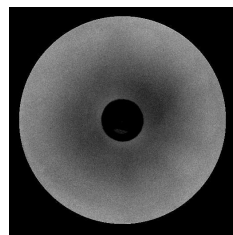
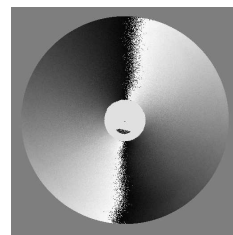


**Figure 3.** Polarization imaging: after being reflected by the mirror, the light becomes partially linearly polarized.



(a)



(b)

**Figure 4.** Images of the polarization parameters that are needed to reconstruct the mirror shape: (a) degree of polarization ( $\rho \in [0, 1]$ ), (b) angle of polarization ( $\varphi \in [0, \pi]$ ).



**Figure 5.** Disambiguation of the azimuth angle: (a) segmented image ( $I_{quad} \in \{0, 1, 2, 3\}$ ), (b) image of the resulting azimuth angle  $\phi$  ( $\phi \in [-\pi/2, 3\pi/2]$ ).

orthographic projection onto the sensor is assumed and the azimuth angle  $\phi$  can be inferred from the angle of polarization  $\varphi$ :

$$\phi = \varphi \pm \frac{\pi}{2}. \quad (4)$$

### 3.2. Disambiguation of the normals

From the equations (3) and (4) the surface normals are determined with an ambiguity. Since mirrors used in catadioptric vision are of convex and revolution shape, a segmented image  $I_{quad}$  can be directly computed from the near center of the mirror (Fig. 5(a)). This segmented image is an image with four gray levels that represent the four quadrants oriented with an angle in  $]0, \pi/2[$ . The algorithm of the disambiguation process described in<sup>16</sup> is applied with the segmented image  $I_{quad}$  and the angle of polarization image  $\varphi$ :

1.  $\phi = \varphi - \frac{\pi}{2}$ ,
2.  $\phi = \phi + \pi$  if  $[(I_{quad} = 0) \wedge (\phi \leq 0)] \vee [I_{quad} = 1] \vee [(I_{quad} = 3) \wedge (\phi \geq 0)]$ ,

where  $\wedge$  and  $\vee$  represent, respectively, the logical operators AND and OR. The result of the disambiguation is presented Fig. 5(b).

### 3.3. Calibration

To calibrate our imaging system, we use the generic calibration concept introduced by Sturm and Ramalingam.<sup>17</sup> The concept considers an image as a collection of pixels, and each pixel measures the light along a particular 3D ray. Thus, calibration is the determination of all projection rays and their correspondence with pixels. A 3d-ray is represented here by a couple of points which belongs to the ray:

$$\mathbf{A} = \begin{bmatrix} x_a \\ y_a \\ z_a \end{bmatrix}, \mathbf{B} = \begin{bmatrix} x_b \\ y_b \\ z_b \end{bmatrix}. \quad (5)$$

To get these points, the 3D surface of the mirror has to be computed. Once the normals are given by polarization imaging, the surface shape of the mirror can be computed thanks to the Frankot-Chellappa algorithm.<sup>18</sup> Denoting by  $f$ ,  $\tilde{p}$  and  $\tilde{q}$  the Fourier transforms of, respectively, the surface height and the  $x, y$  gradients, we have:

$$\forall (u, v) \neq (0, 0), \tilde{f}(u, v) = \frac{-ju\tilde{p} - jv\tilde{q}}{u^2 + v^2}. \quad (6)$$

The three-dimensional surface is obtained by taking the inverse Fourier transform of the former equation. This integration process gives us the surface height of the mirror with a constant of integration. Nevertheless, this constant is not required since the orthographic projection is assumed. To calibrate the sensor, let us take the point  $\mathbf{A} = [x, y, z]^T$ , that both belongs to the mirror surface and the 3D-ray, be the first point of the ray (Fig. 3). The second point  $\mathbf{B}$  of the ray can be written as:

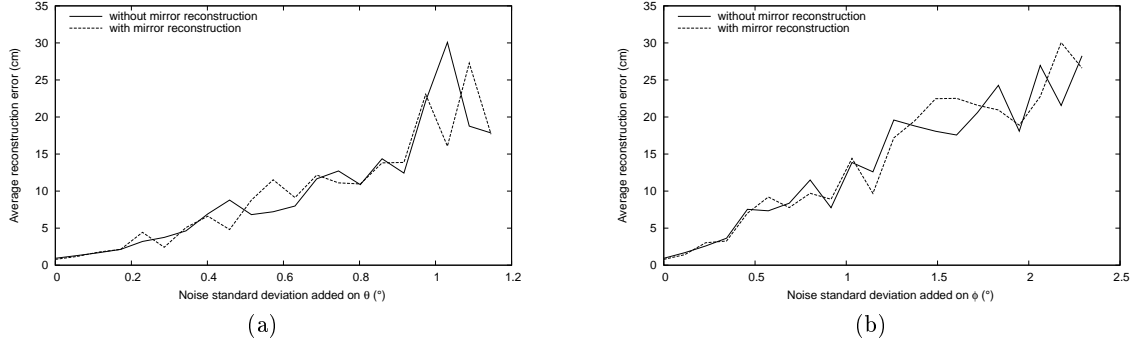


**Figure 6.** Reconstruction error induced by noisy measurement of the normals parameters: (a)  $\theta$  angle, (b)  $\phi$  angle.

$$\mathbf{B} = \mathbf{A} + k \begin{bmatrix} \tan 2\theta \cos \phi \\ \tan 2\theta \sin \phi \\ 1 \end{bmatrix}, \quad (7)$$

where  $k$  is a non-null constant.

## 4. EXPERIMENTS

In the previous section, we show that the three-dimensional parameters of the mirror ( $z$ ,  $\theta$ ,  $\phi$ ) are required to calibrate the catadioptric system according to the generic calibration concept introduced by Sturm.  $z$  represents the mirror height,  $\theta$  and  $\phi$  represent respectively the azimuth and zenith angles of the normals. In this section, simulations are firstly presented to illustrate the influence of the parameters on the reconstruction quality. Then, preliminary results on a calibrated spherical mirror show a good accuracy of the three-dimensional parameters measurement by polarization imaging.

### 4.1. Simulations

To simulate the three-dimensional reconstruction error, the normals angles  $\theta$  and  $\phi$  were computed from a perfect parabolic mirror with a  $7^\circ$  misalignment from the camera optical axis. The parameters are then disturbed by gaussian noise. The synthetic scene introduced in section 2 is reconstructed thanks to the generic calibration concept. Figure 6(a) and Figure 6(b) show respectively reconstruction error of the scene induced by noisy measurement of  $\theta$  and  $\phi$ . The synthetic scene is reconstructed with or without the mirror reconstruction meaning that the integration process from equation (6) is carried out or not. Figure 6 shows, on the one hand, that the scene reconstruction is quite sensitive to the measurement of the parameters  $\theta$  and  $\phi$ . On the other hand, the integration process is not required, and we can assume that the  $z$  parameter is negligible.

In addition, Figure 7 shows reconstruction error of the scene by only adding gaussian noise to the  $z$  mirror height. The reconstruction quality remains good even if the mirror height is very noisy (the mirror height is  $1cm$  and the radius is  $2cm$ ).

### 4.2. Preliminary results

Preliminary results were carried out with a catadioptric sensor made of a camera with a telecentric lens and a calibrated spherical mirror ( $radius = 1cm$ ). Let us notice that our system did not satisfy the single view point constraint. Nevertheless this property is not required here for the three-dimensional reconstruction of the scene. As described in section 3, our catadioptric sensor is calibrated by measuring the three-dimensional parameters of the mirror with a liquid crystal polarization rotator placed between the camera and the mirror. To evaluate the accuracy of our system, we compare the parameters ( $\theta$ ,  $\phi$  and  $z$ ) obtained with our system to the theoretical parameters of the mirror (Figure 8).

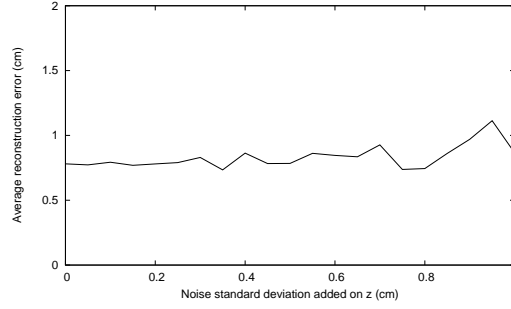


**Figure 7.** Reconstruction error induced by noisy calculation of the mirror height  $z$ .

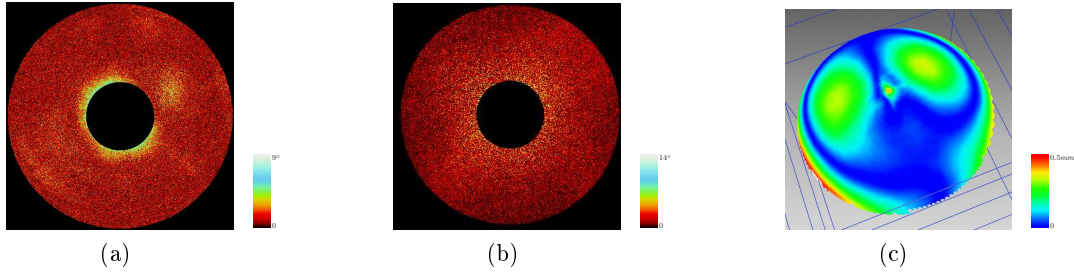


**Figure 8.** Measurement errors of the three-dimensional parameters: (a) angle  $\theta$ , (b) angle  $\phi$  and (c) deviation map of the mirror  $z$ .

The mean quadratic errors of the angles  $\theta$  and  $\phi$  are respectively  $0.49^\circ$  and  $1.02^\circ$ . Figure 9 shows the reconstruction of the synthetic scene by taking the calibration made by polarization imaging. Since the mirror is spherical, three-dimensional reconstruction errors increase highly. Nevertheless, the synthetic scene is well reconstructed with an average error of  $9.68cm$ .

## 5. CONCLUSION

In this paper, a new efficient calibration method for catadioptric sensors has been presented. This method is based on the three-dimensional parameters measurement of the mirror thanks to polarization imaging. The calibration can be performed “in one click” even by a non-specialist as it only requires an optical apparatus, no image processing and no calibration pattern. Contrary to traditional methods, it deals with misalignment

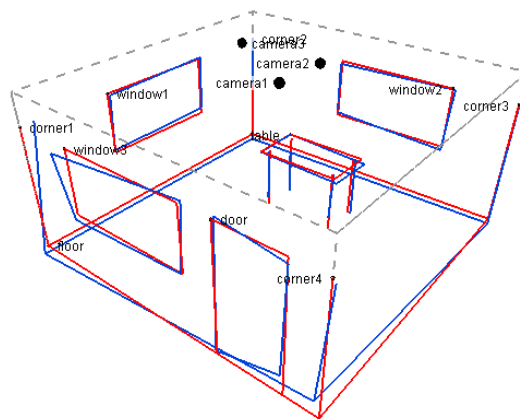


**Figure 9.** Simulation of the three-dimensional reconstruction by using the calibration done from the polarization imaging.

of the sensor and work for any shape of mirror (regular or not). Experimental results prove that the sensor is properly calibrated and a satisfactory three-dimensional reconstruction of the scene can be obtained. We have also shown that the 3D-shape of the mirror can be neglected in comparison with the normals orientations. The platform3D department is currently manufacturing a parabolic mirror and future work will consist in creating a paracatadioptric sensor in order to compare our method to other methods known in the literature on real scenes.

## REFERENCES

1. S. Baker and S. K. Nayar, "A theory of catadioptric image formation," in *International Conference on Computer Vision*, pp. 35–42, IEEE Computer Society, (Washington, DC, USA), 1998.
2. P. Sturm, "Multi-view geometry for general camera models," in *IEEE Computer Vision and Pattern Recognition*, **1**, pp. 206–212, IEEE Computer Society, (Washington, DC, USA), 2005.
3. S. Ramalingam, S. K. Lodha, and P. Sturm, "A generic structure-from-motion framework," *Computer Vision and Image Understanding* **103**, pp. 218–228, September 2006.
4. Y. Yagi, S. Kawato, and S. Tsuji, "Real-time omnidirectional image sensor (copis) for vision-guided navigation," *IEEE Trans. Robotics and Automation* **10**, pp. 11–22, February 1994.
5. S. Kang, "Catadioptric self-calibration," in *IEEE Computer Vision and Pattern Recognition*, pp. 1201–1207, 2000.
6. C. Geyer and K. Daniilidis, "Paracatadioptric camera calibration," *IEEE Trans. Pattern Analysis and Machine Intelligence* **24**(5), pp. 687–695, 2002.
7. J. P. Barreto and H. Araujo, "Paracatadioptric camera calibration using lines," *International Conference on Computer Vision* **02**, pp. 1359–1365, 2003.
8. B. Vanderportaele, M. Cattoen, P. Marthon, and P. Gurdjos, "A new linear calibration method for paracatadioptric cameras," *International Conference on Pattern Recognition* **4**, pp. 647–651, 2006.
9. M. D. Grossberg and S. K. Nayar, "A general imaging model and a method for finding its parameters," in *International Conference on Computer Vision*, **2**, pp. 108–115, 2001.
10. R. Pless, "Using many cameras as one," in *IEEE Computer Vision and Pattern Recognition*, **2**, pp. 587–593, 2003.
11. L. B. Wolff, "Polarization-based material classification from specular reflection," *IEEE Trans. Pattern Analysis and Machine Intelligence* **12**, pp. 1059–1071, November 1990.
12. S. Rahmann, "Reconstruction of quadrics from two polarization views," in *Iberian Conference on Pattern Recognition and Image Analysis (IbPRIA03)*, Springer, LNCS 2652, Mallorca, Spain, pp. 810–820, June 2003.
13. D. Miyazaki, M. Kagesawa, and K. Ikeuchi, "Transparent surface modeling from a pair of polarization images," *IEEE Trans. Pattern Analysis and Machine Intelligence* **26**, pp. 73–82, January 2004.
14. L. B. Wolff and T. E. Boult, "Constraining object features using a polarization reflectance model," *IEEE Trans. Pattern Analysis and Machine Intelligence* **13**, pp. 635–657, July 1991.
15. O. Morel, C. Stolz, F. Meriaudeau, and P. Gorria, "Three-dimensional inspection of highly-reflective metallic objects by polarization imaging," *Electronic Imaging Newsletter* **15**(2), p. 4, 2005.
16. O. Morel, C. Stolz, F. Meriaudeau, and P. Gorria, "Active lighting applied to 3d reconstruction of specular metallic surfaces by polarization imaging," *Applied Optics* **45**, pp. 4062–4068, June 2006.
17. P. Sturm and S. Ramalingam, "A generic concept for camera calibration," in *European Conference on Computer Vision*, **2**, pp. 1–13, Springer, (Prague, Czech Republic), May 2004.
18. R. Frankot and R. Chellappa, "A method for enforcing integrability in shape from shading algorithms," *IEEE Trans. Pattern Analysis and Machine Intelligence* **10**, pp. 439–451, July 1988.